JOURNAL OF PROPULSION AND POWER
Vol. 9, No. 1, Jan.–Feb. 1993

Wake Ingestion Propulsion Benefit

Leroy H. Smith Jr.*
GE Aircraft Engines, Cincinnati, Ohio 45215

It is well-known that the efficiency of propulsion is improved if part or all of the propulsive fluid comes from the wake of the craft being propelled. In this article this propulsion benefit is quantified in terms of wake parameters and propulsor properties. The formulations apply directly to unducted fans or propellers, but the conclusions are also relevant to ducted propulsors. It is found that the power saving is greatest when the propulsor disk loading is high, when the wake form factor is high (flow near separation), and when the propulsor design is such that the wake profile tends to be flattened as it passes through the propulsor (high wake recovery). Examples are given showing that the benefit can be in the 20% range in some cases. Propeller design parameters that lead to high wake recovery are also given.

Nomenclature

A = propulsor disk area, Figs. 3 and 17
C_T = local thrust coefficient, $(T/A)/\frac{1}{2}\rho U^2$
C_{Th} = thrust-loading coefficient, $T/\frac{1}{2}\rho V_0^2 A$
c = blade chord
D = viscous drag of the part of the craft whose wake is to be ingested
H = wake form factor, Eq. (14)
K = wake pseudoenergy factor, Eq. (15)
k = wake pseudoenergy area, Eq. (11)
$\dot{m}$ = mass flow rate through the propulsor
P = shaft power
P_p = propulsive power, Eqs. (4) and (21)
PSC = power-saving coefficient, Eq. (23)
P_T = total (stagnation) pressure
p = static pressure
R = wake recovery, Fig. 3, Eq. (16)
s = blade circumferential spacing
T = total propulsive thrust of the propulsor system. This includes any thrust or drag pressure forces on the craft that are induced by the action of the propulsor.
U = local blade speed
V = velocity relative to the craft being propelled
V_j = axial velocity in the jet; axial means the freestream flow direction
y = distance across wake
Δ = wake velocity defect, Fig. 3
δ = wake area, Fig. 3
δ^* = wake displacement area, Eq. (9)
η = propulsor efficiency, V_0T/P
η_{KE} = axial kinetic energy efficiency, Eq. (7)
η_p = propulsive efficiency, Eq. (5) and footnote
θ = wake momentum area, Eq. (10)
ν = cascade deviation coefficient, Eq. (58)
ρ = fluid density
σ = cascade solidity, c/s
φ = flow angle measured from circumferential direction, Fig. 12
φ^* = cascade zero-lift direction, Fig. 12
ϕ = local advance coefficient, V_0/U
ψ = stream function, Fig. 17

Subscripts

j = in far downstream jet, in freestream direction
p = at the propulsor disk, except when defined above
t = at propulsor tip
u = in circumferential direction
w = in wake
wp = wake propulsion ideal case
0 = far upstream; in freestream; ambient
1 = immediately ahead of propulsor disk
2 = immediately behind propulsor disk

Superscript

$'$ = wake not ingested by propulsor

I. Introduction

IT has long been known in the field of marine propulsion that the propulsive efficiency is improved when fluid from the wake of the craft is used as part or all of the propulsive stream. Betz[1] explains this and points out that with wake ingestion the power expended can actually be less than the product of the forward speed and craft drag. Wislicenus and Smith,[2] Wislicenus,[3] Gearhart and Henderson,[4] and Bruce et al.[5] conducted design studies of propulsors employing wake ingestion aimed mainly at the propulsion of submerged bodies; wake-adapted propulsors are commonplace for torpedo and other marine applications.

For aircraft propulsion, wake ingestion appears somewhat less beneficial. With wings the wake is spread out, so it is harder to capture a substantial portion of it with the propulsor. Another drawback is the reduced density and total pressure of the air in the wake; this is mainly a disadvantage to the core engine which is desupercharged and, therefore, has to be made larger. However, there are aircraft applications where wake ingestion is clearly beneficial. One of these is the cruise missile where the concentric aft-located single-engine propulsor can capture most of the body wake, and a bottom inlet can supply the core engine with largely unspoiled air. Unpublished studies of unducted fan propulsors on cruise missiles have shown at least a 7% power reduction due to wake ingestion. The author thinks it is likely that other worthwhile applications can be found.

Another category in which wake ingestion is of interest is in the treatment of the drag of appendages such as support struts or control surfaces. If the appendage wake fluid passes through the propulsor, part of the drag is offset by an improvement in propulsive efficiency, with a likely benefit for the system as a whole.

Presented as Paper 91-2007 at the AIAA/ASME/SAE 27th Joint Propulsion Conference, Sacramento, CA, June 24–27, 1991; received July 25, 1991; revision received July 9, 1992; accepted for publication July 31, 1992.

This article is dedicated to the memory of George Wislicenus, who had a lifelong interest in this subject, and who was responsible for the author's early interst in it.

*Consulting Technologist, Turbomachinery Aerodynamics, 1 Neumann Way, M/D A323.

The wake ingestion propulsion benefit will be quantified in two ways. First, a power-saving coefficient will be defined. This is most relevant to the appendage category of cases. Then a propulsive efficiency with wake ingestion will be derived; this will be of greater interest when a substantial portion of the propulsor thrust comes from the propelled craft's wake fluid.

II. Analysis

A. Propulsor Without Wake Ingestion

The basic model used for analysis is the simple classical actuator disk shown in Fig. 1. For this model the density is uniform, the flow is axisymmetric, the static pressure far removed from the disk is uniform at the ambient value, there are no viscous forces or mixing at the edges of the jet, and properties across the jet are uniform. With this model it can be shown (e.g., McCormick[6]) that the axial velocity at the propulsor disk is the mean of the far upstream and far downstream values

$$V_p = [(V_j + V_0)/2] \tag{1}$$

The thrust is the mass flow times the increase in axial velocity

$$T = \dot{m}(V_j - V_0) \tag{2}$$

$$= \rho A V_p (V_j - V_0) \tag{3}$$

The propulsive power is defined as the mass flow times the increase in axial kinetic energy of the fluid

$$P_p = \dot{m}[(V_j^2/2) - (V_0^2/2)] \tag{4}$$

The propulsive efficiency [The author has been unable to locate a universally accepted definition for the term "propulsive efficiency." The definition adopted here is similar to that used by Wislicenus[3] and Gearhart and Henderson[4] except losses caused by casing external surfaces and downstream swirl have not been included. Since with wake ingestion the propulsive efficiency can be greater than unity, it is sometimes called "propulsive coefficient." In the definition of propulsive efficiency used by naval architects, the numerator contains the total craft resistance (which equals T herein), and the denominator is the full shaft power; therefore it matches the propulsor efficiency defined herein by Eq. (8).]

$$\eta_p = (V_0 T / P_p) \tag{5}$$

becomes for this case, using Eqs. (2) and (4), the well-known Froude efficiency

$$\eta_p = [2V_0/(V_j + V_0)] \tag{6}$$

In applying this model to an actual case at a given thrust it is necessary to recognize that the actual shaft power is greater than the propulsive power for several reasons:

1) The flow through the propulsor will incur viscous losses and, perhaps, shock losses.

2) Some of the kinetic energy in the jet may not be axial. This is certainly the case if the propulsor is a single-rotation propeller.

3) With a finite number of blades, a propeller will have an induced loss.

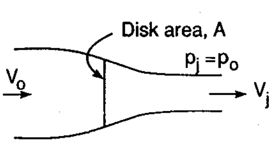

Fig. 1 Actuator disk propulsor.

We incorporate all of these reasons into another efficiency relating the propulsive power P_p to the actual shaft power P

$$\eta_{KE} = \frac{\dot{m}[(V_j^2/2) - (V_0^2/2)]}{P} \tag{7}$$

and the overall propulsor efficiency then is

$$\eta = (V_0 T/P) = \eta_p \eta_{KE} \tag{8}$$

In this article the focus will be on propulsive efficiency effects. It is therefore tacitly assumed that η_{KE} is more or less unchanged when a wake is ingested into a given type of propulsor. This assumption is supported by the following private communication to the author from William B. Morgan, Head—Ship Hydrodynamics Department, David Taylor Research Center:

> In general, one can say that wake flow non-uniformities of the type from a good ship design do not cause additional losses. Of course, if the wake is extremely non-uniform, separation could possibly occur on the blades with a loss in efficiency. It is common to design the propeller for a circumferentially averaged wake and then to calculate the efficiency on this basis. Numerous experiments have shown that the efficiency is accurately predicted by this method even though the ship's wake is non-uniform. This convinces me, except for extreme non-uniformity, that a non-uniform wake does not cause any measurable loss in efficiency.

This view is also supported by the author's experience with fans and compressors.

B. Wake Properties

Figure 2 shows a body and its viscous wake. For the purpose of identifying wake properties we specify that the static pressure across the wake is constant at the ambient value. This removes potential field effects so that the wake will be directly related to viscous drag. This will be discussed further in Sec. V.

The following wake integral properties will be employed in the analysis:

Wake displacement area

$$\delta^* = \int^{\delta} \left(1 - \frac{V_w}{V_0}\right) dA \tag{9}$$

Wake momentum area

$$\theta = \int^{\delta} \frac{V_w}{V_0} \left(1 - \frac{V_w}{V_0}\right) dA \tag{10}$$

Wake pseudoenergy area

$$k = \int^{\delta} \frac{V_w^2}{V_0^2} \left(1 - \frac{V_w}{V_0}\right) dA \tag{11}$$

where dA is an area element at the plane where the integrals are being evaluated. Analysis of a control volume containing

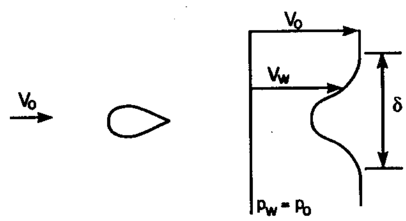

Fig. 2 Body and wake.

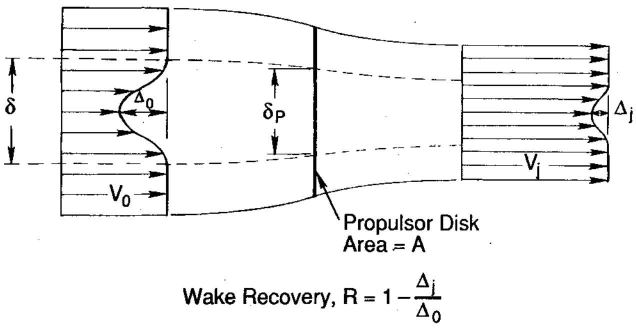

Fig. 3 Propulsor ingesting wake.

the body gives us the body drag

$$D = \rho \int^{\delta} V_w(V_0 - V_w)\, dA \tag{12}$$

Using Eq. (10) this is

$$D = \rho V_0^2 \theta \tag{13}$$

Wake shape parameters that will be used are

Form factor

$$H = (\delta^*/\theta) \tag{14}$$

Pseudoenergy factor

$$K = (k/\theta) \tag{15}$$

C. Propulsor with Wake Ingestion

Figure 3 shows a wake passing through the actuator disk propulsor. For the analysis the wake fluid maintains its identity and viscous shear stresses are neglected. The flattening of the wake is measured by the wake recovery R as defined in Fig. 3. The wake *is* flattened (R is greater than zero) for two reasons: 1) a propulsor has a natural tendency to add more energy to fluid that approaches it with lower axial velocity; and 2) even if the propulsor added the same energy to the wake fluid as it did to the rest of the propulsor stream, its axial velocity defect would be reduced so as to keep the same kinetic energy defect. The actual value of R depends on many propulsor parameters, some of which will be evaluated later. For now, we keep R in the analysis as an independent parameter. Also, for simplicity we assume that R has the same value for all wake streamlines, not just the wake center streamline shown in Fig. 3. Thus

$$R = 1 - [(V_j - V_{jw})/(V_0 - V_w)] \tag{16}$$

is a constant for all wake streamlines.

It will be convenient to employ a wake displacement thickness at the propulsor face even though the static pressure is not uniform there. With constant density the wake fluid volume flow is the same at the propulsor face as it is far upstream. Therefore

$$V_p(\delta_p - \delta_p^*) = V_0(\delta - \delta^*) \tag{17}$$

Employing Eq. (1) this becomes

$$[(V_j + V_0)/2](\delta_p - \delta_p^*) = V_0(\delta - \delta^*) \tag{18}$$

The propulsor thrust is the sum of the thrusts produced by the nonwake and the wake fluid streams

$$T = \rho(A - \delta_p)\frac{V_j + V_0}{2}(V_j - V_0) + \rho \int^{\delta} V_w(V_{jw} - V_w)\, dA \tag{19}$$

where dA is an area increment upstream where the integral is evaluated. To evaluate Eq. (19), δ_p is obtained from Eq. (18) and V_{jw} is obtained from Eq. (16). Also using Eqs. (9), (10), and (13), Eq. (19) can be simplified to

$$T = (\rho/2)(A - \delta_p^*)(V_j^2 - V_0^2) + RD \tag{20}$$

In a similar fashion the propulsor propulsive power

$$P_p = \rho(A - \delta_p)\frac{V_j + V_0}{2}\left(\frac{V_j^2}{2} - \frac{V_0^2}{2}\right) + \rho \int^{\delta} V_w \left(\frac{V_{jw}^2}{2} - \frac{V_w^2}{2}\right) dA \tag{21}$$

is evaluated using also Eqs. (11), (15), and (20), and after considerable algebra we obtain

$$P_p = \tfrac{1}{2}\{T(V_j + V_0) - DV_0(2 - R)[(V_j/V_0) - 1 + R(1 - K)]\} \tag{22}$$

D. Power-Saving Coefficient

Consider that the body shedding the wake to be ingested has a certain drag D; an equal thrust must be provided to propel it. In one case its wake goes through the propulsor, and in another case it does not. We postulate that the propulsor disk area is the same in both cases. Anticipating that the propulsive power will be less when the wake is ingested, we define a power-saving coefficient

$$\mathrm{PSC} = \frac{P_p' - P_p}{V_0 D/\eta_p'} \tag{23}$$

where the prime denotes the case when the wake is not ingested. The denominator of Eq. (23) is seen to be the propulsive power required to propel the body when the wake is not ingested.

The power saving coefficient is defined in terms of propulsive powers. If we assume that η_{KE} is the same with and without wake injestion, then it can also be applied to shaft powers; this can be seen by dividing both the numerator and denominator of Eq. (23) by η_{KE}.

The total propulsor thrust T, made up of D plus whatever other thrust is needed, is the same for both cases:

$$T' = T \tag{24}$$

For the case when the wake is not ingested, Eqs. (20) and (22) simplify to

$$T' = (\rho/2)A(V_j'^2 - V_0^2) \tag{25}$$

$$P_p' = \tfrac{1}{2}T'(V_j' + V_0) \tag{26}$$

Substituting Eqs. (26) and (22) into Eq. (23), using Eq. (24) and also using Eq. (6) with primes added, the power-saving coefficient becomes

$$\mathrm{PSC} = [(V_j' - V_j)/(V_j' + V_0)](T/D) + \{[V_0(2 - R)]/(V_j' + V_0)\}[(V_j/V_0) - 1 + R(1 - K)] \tag{27}$$

Further manipulations are needed to express V_j' in terms of V_j and other convenient variables. Substituting Eqs. (25) and (20) into Eq. (24) and employing Eq. (13) we obtain

$$V_j'^2 = V_j^2 + 2V_0^2(\theta/A)R - (V_j^2 - V_0^2)(\delta_p^*/\theta)(\theta/A) \tag{28}$$

Manipulation of Eq. (20) using Eq. (13) leads to

$$\frac{\theta}{A} = \frac{\tfrac{1}{2}(D/T)[(V_j^2/V_0^2) - 1]}{1 - R(D/T) + \tfrac{1}{2}(D/T)[(V_j^2/V_0^2) - 1](\delta_p^*/\theta)} \tag{29}$$

In order to determine δ_p^*, we study the deformation of the wake as it reaches the disk. The actuator disk result already given by Eq. (1) can be applied to the individual wake streamlines

$$V_{pw} = [(V_{jw} + V_w)/2] \tag{30}$$

Then, using Eq. (16), we find

$$V_p - V_{pw} = [(2 - R)/2](V_0 - V_w) \tag{31}$$

By definition

$$V_p\delta_p^* = \int^{\delta_p} (V_p - V_{pw})\, \mathrm{d}A_p \tag{32}$$

Using Eq. (31)

$$V_p\delta_p^* = \frac{2-R}{2}\int^{\delta_p} (V_0 - V_w)\, \mathrm{d}A_p \tag{33}$$

Now

$$\int^{\delta_p} (V_0 - V_w)\, \mathrm{d}A_p \doteq \frac{\delta_p}{\delta}\int^{\delta} (V_0 - V_w)\, \mathrm{d}A \tag{34}$$

for shallow wakes. It is necessary to assume shallow wakes so that $\mathrm{d}A/\mathrm{d}A_p$ will be nearly constant for all stream-tubes, otherwise Eq. (34) is not strictly true. Using Eqs. (34) and (9), Eq. (33) then yields

$$\delta_p^* = \delta^*[(2 - R)/2](V_0/V_p)(\delta_p/\delta) \tag{35}$$

Further manipulations using Eqs. (1), (14), and (17) lead to

$$\frac{\delta_p^*}{\theta} = \frac{2H(2 - R)V_0^2}{(V_j + V_0)^2}\;\frac{1 - \dfrac{\delta^*}{\delta}}{1 - \dfrac{(2 - R)V_0}{V_j + V_0}\dfrac{\delta^*}{\delta}} \tag{36}$$

$$(A/\delta_p) = (\theta/\delta_p^*)(A/\theta)\{[(2 - R)V_0]/(V_j + V_0)\}(\delta^*/\delta) \tag{37}$$

With Eqs. (27–29) and (36) we have the power-saving coefficient expressed in terms of

- R = a measure of the blading capability to attenuate wakes
- V_j/V_0 = a measure of the disk loading
- D/T = a measure of the wake quantity being considered
- H, K, δ^*/δ = measures of the wake shape

For small values of D/T, $V_j' - V_j$ is nearly zero and the first term in Eq. (27) becomes indeterminent. This case is treated in the Appendix.

For presentation of results, a thrust-loading coefficient will be used to represent disk loading

$$C_{\mathrm{Th}} = (T/\tfrac{1}{2}\rho V_0^2 A) \tag{38}$$

Using Eqs. (24) and (25) this is also

$$C_{\mathrm{Th}} = (V_j'^2/V_0^2) - 1 \tag{39}$$

E. Propulsive Efficiency with Wake Ingestion

The concept of propulsive efficiency is the same whether or not there is wake ingestion; therefore, Eq. (5) still applies. Using it with Eq. (22) yields

$$\eta_p = \frac{2}{\dfrac{V_j}{V_0} + 1 - \dfrac{D}{T}(2 - R)\left[\dfrac{V_j}{V_0} - 1 + R(1 - K)\right]} \tag{40}$$

As explained in Sec. II.A., in order to obtain the overall propulsor efficiency, which is based on shaft power, it is necessary to multiply η_p by η_{KE}, which is the efficiency for converting shaft power into jet axial kinetic energy flux.

F. Special Case: Wake Propulsion Ideal

For a case when all of a craft's drag is viscous drag, the highest propulsive efficiency will be attained when only wake fluid passes through the propulsor, and when each streamline has its axial velocity brought back up to the freestream value. We call this the wake propulsion ideal case, and for it we have

$$\delta_p = A, \quad R = 1, \quad V_j = V_0 = V_p, \quad T = \mathrm{D} \tag{41}$$

Using Eqs. (41), Eq. (27) becomes

$$\mathrm{PSC}|_{wp} = [V_0/(V_j' + V_0)][(V_j'/V_0) - K] \tag{42}$$

and using Eq. (39) this becomes

$$\mathrm{PSC}|_{wp} = [(\sqrt{1 + C_{\mathrm{Th}}} - K)/(\sqrt{1 + C_{\mathrm{Th}}} + 1)] \tag{43}$$

With $\delta_p = A$, $T = \rho V_0^2\theta$, and $\theta = \delta^*/H$, Eq. (38) becomes

$$C_{\mathrm{Th}}|_{wp} = (2/H)(\delta^*/\delta_p) \tag{44}$$

Using also Eqs. (18) and (36), Eq. (44) can be manipulated to

$$C_{\mathrm{Th}}|_{wp} = \frac{(\delta^*/\delta)[2 - (\delta^*/\delta)]}{H[1 - (\delta^*/\delta)]} \tag{45}$$

This interesting result shows that for the wake propulsion ideal case the thrust-loading coefficient depends only on wake-shape parameters. Furthermore, substitution of Eq. (45) into Eq. (43) gives an expression for the power-saving coefficient that depends only on wake-shape parameters.

Using Eqs. (41), Eq. (40) becomes

$$\eta_p|_{wp} = [2/(1 + K)] \tag{46}$$

a very simple expression for the propulsive efficiency for the wake propulsion ideal case.

G. Wake-Shape Parameter Evaluation

The preceeding analyses led to results that contain three wake-shape parameters, H, K, and δ^*/δ, with K apparently playing the most significant role. Since K is not a widely used parameter, it will be helpful if we can relate it to the more familiar form factor H. Fortunately, work was done on this in the 1950s at NACA, and Fig. 4 from Lieblein and Roude-

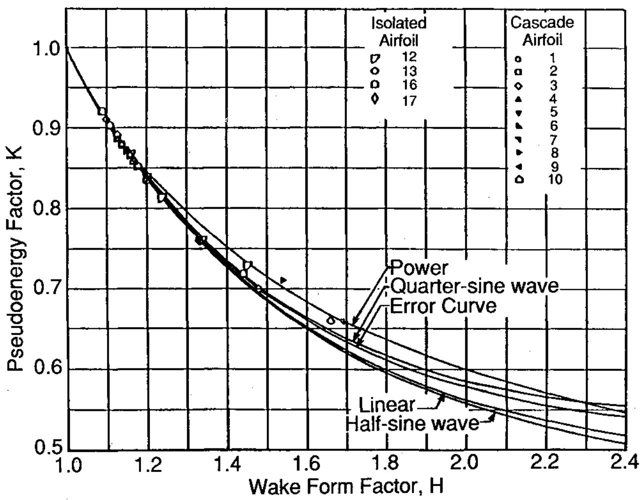

Fig. 4 Pseudoenergy factor data for airfoil wakes, Ref. 7.

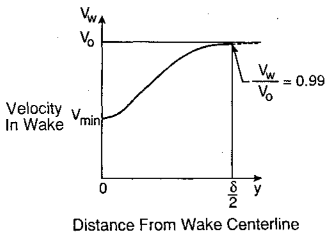

Fig. 5 Error curve wake profile.

bush,[7] gives a correlation for two-dimensional airfoil wakes. Also shown in Fig. 4 are the results for several analytical wake representations, and it could be argued that any of them fits the data adequately. For our purposes we adopt the error curve shape (Fig. 5). Its analytical representation is (Lieblein and Roudebush[7])

$$(V_w/V_0) = 1 - [1 - (V_{min}/V_0)]\exp[-b_1(2y/\delta)^2] \quad (47)$$

where

$$b_1 = \ln\{100\sqrt{2}[1 - (V_{min}/V_0)]\}$$

For this shape the pseudoenergy factor is

$$K = (1/H)[(a - 1)H^2 - 2(a - 1)H + a] \quad (48)$$

where

$$a = (2/\sqrt{3})$$

and the displacement thickness ratio is

$$(\delta^*/\delta) = \sqrt{(\pi/2b)}[(H - 1)/H] \quad (H > 1.1) \quad (49)$$

$$= 0 \quad (H = 1)$$

where

$$b = \ln\{100\sqrt{2}[(H - 1)/H]\}$$

Equations (48) and (49) will be used for simplicity when the numerical results presented in Sec. III are generated, even though such a tight correlation as shown in Fig. 4 would probably not be found for three-dimensional body wakes.

III. Numerical Results

A. Power-Saving Coefficient Evaluation

The calculation procedure is as follows: Three of the independent variables R, D/T, and H are given, and several values of V_j/V_0 are also specified. Eqs. (48), (49), (36), (29), (28), and (27) are then applied to obtain power saving coefficient values. The corresponding thrust-loading coefficients are calculated from Eq. (39). Eq. (37) is evaluated, and cases for which $A/\delta_p < 1$ are eliminated because they violate the assumptions of the model shown in Fig. 3.

Figure 6 was constructed for cases where the body drag is much less than the propulsor thrust. A case in point is the support strut for an unducted fan engine aft-mounted on an aircraft fuselage. With this case in mind, the abscissa scale has been double-labeled for typical GE36 operating points. It appears that perhaps 15–20% of the strut drag would be recovered at high Mach operation depending on the wake form factor.

The dependency of PSC on H has physical significance. As viscous wakes move downstream, shear stresses tend to flatten them. This reduces their form factor and less power will be saved. The message here is that, to maximize efficiency, the propulsor should be positioned to ingest a viscous wake before the wake has had much time to dissipate. The same phenomenon is thought to partially explain the experimental obser-

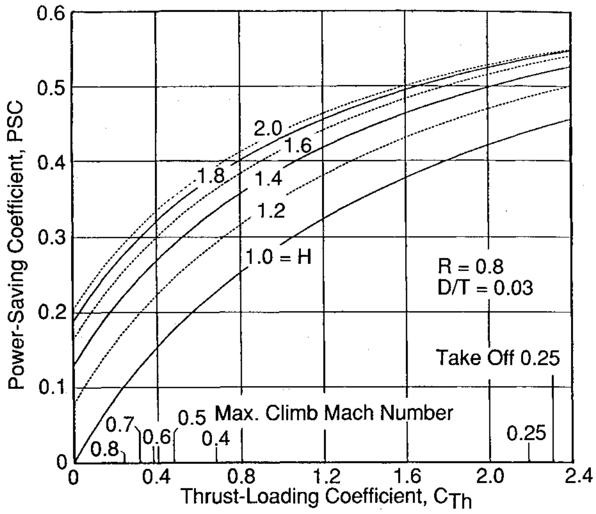

Fig. 6 Effects of disk loading and wake form factor on power required to propel that part of the craft whose wake is being ingested.

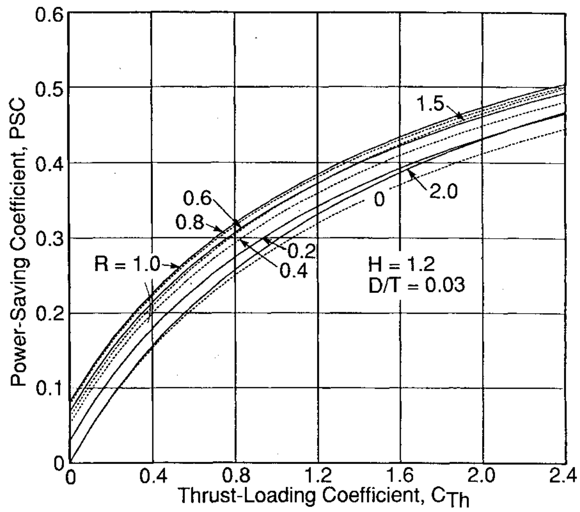

Fig. 7 Effect of wake recovery.

vation that multistage turbomachines have improved performance when the axial gaps between blade rows are reduced.

Figure 6 also provides help in estimating the improved installed performance of a wing-mounted pusher propeller that acts on the wake fluid of part of the wing compared to that of a tractor propeller whose wash increases the drag of the wing.

The ability of a propulsor to add more energy to the low velocity parts of a wake and thus recover the flow to a more uniform state is measured by the propulsor's wake recovery R, defined in Fig. 3. In Fig. 7 R has been varied over a wide range. As expected, the power saving is greatest when $R = 1$, the case for which the jet is uniform. It is remarkable, however, that the recovery can differ significantly from unity without the power saving being much affected. This is fortunate because an accurate prediction of R for a given propulsor is difficult. Approximate methods for estimating R for propeller-type propulsors are given in Sec. IV.

As defined, the power-saving coefficient is normalized by the power required to propel the body (or the part of the body) whose wake is to be ingested. In the two preceeding figures, that power was small compared to that of the whole propulsor, since $D/T = 0.03$. In Fig. 8 we also consider cases for which a large part of the total craft wake is ingested. The curves are terminated at the thrust-loading coefficients for which the disk areas have become small enough that they equal the wake areas. When $D/T = 1$, all of the craft's wake passes through the propulsor, whose thrust just equals the craft's viscous drag; for this case PSC is a fraction of roughly all of the power and so its numerical values are lower. For such cases it is usually more useful to employ the propulsive efficiency with wake ingestion, rather than the power-saving coefficient, to estimate power savings. This is done in the following section.

B. Propulsive Efficiency Evaluation

We proceed as in the previous section, specifying R, D/T, and H values and a range of V_j/V_0. Equation (40) is used to calculate η_p, and Eq. (39) is used for C_{Th}, limited by Eq. (37).

For the examples shown in Fig. 9, H is set at 1.3, which may be representative for craft such as cruise missiles. R is 0.8, which is probably attainable for most propulsors designed for wake adaptation except single-rotation propellers. But to show that the efficiency is not very sensitive to R, R has also been given other values for $D/T = 0.4$. The effect of R is somewhat greater for larger D/T values.

The $D/T = 0$ curve in Fig. 9, which applies when no wake is ingested, is the familiar Froude efficiency variation showing a significant loss in efficiency as the propulsor is made smaller. But when a large part of the craft's wake is ingested by the propulsor, there is much less incentive to keep the propulsor large. The message here is that, for best efficiency the propulsor should be positioned and sized to ingest as much wake fluid as possible (increase D/T), but after that, making it still larger does not pay off in propulsive efficiency and would have other adverse effects such as increased weight.

C. Wake Propulsion Ideal Case Evaluation

The analysis presented in Sec. II.F for this case, where the propulsor just restores the momentum defect in the wake to

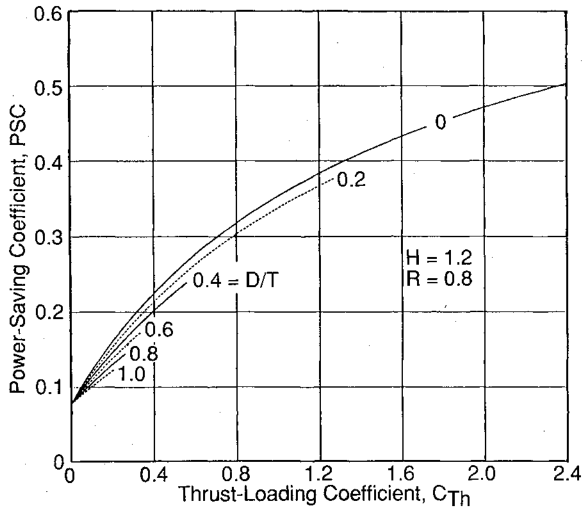

Fig. 8 Effect of quantity of wake being ingested.

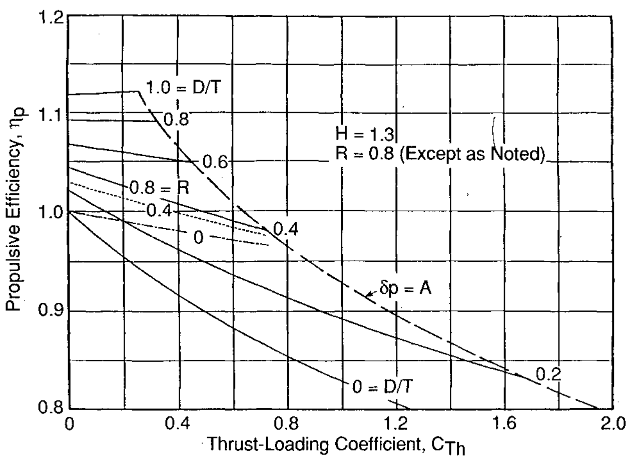

Fig. 9 Propulsive efficiency gains from wake ingestion.

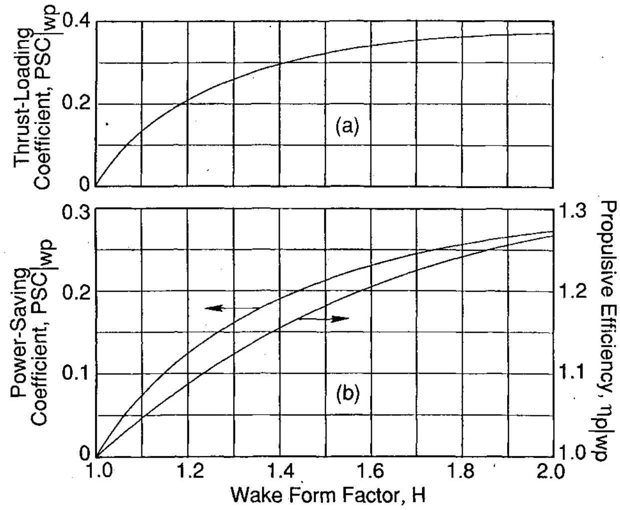

Fig. 10 Wake propulsion ideal case.

produce a thrust just equal to the drag, indicated that the thrust-loading coefficient of such an ideal propulsor depends only on wake-shape parameters. This relationship [Eq. (45)] is shown in Fig. 10a. The corresponding ideal power saving coefficient [Eq. (43)] and ideal propulsive efficiency, [Eq. (46)] are shown in Fig. 10b. The potential power saving is seen to be quite significant. Figure 10 again emphasizes the benefit of placing the propulsor forward in the wake where the form factor is highest. The benefit is not only in efficiency, but also, as Fig. 10a indicates, in reduced propulsor size.

IV. Wake Recovery Evaluation

For a wake-adapted propulsor design, which would be done for a cruise missile or torpedo, the blading can be shaped to assure a good wake recovery (except for a single-rotation propeller where hub swirl could not be removed; unless part-span stator vanes ahead of or behind the propeller are employed).

However, for circumferentially varying wakes (such as the strut wake that was described in connection with Fig. 6) it is not obvious what the wake recovery might be. Although it was shown that the power-saving coefficient and propulsive efficiency are not very sensitive to wake recovery, some method for estimating it is needed short of detailed calculations of the flow in the propulsor blading. Some approximations are therefore developed in this section using a simplified actuator disk approach that neglects upstream-induced swirl velocities.

A. Element Characteristic Slope

For each radial element of a propulsor the characteristic diagram shown in Fig. 11 can be drawn. Here C_T is the local thrust coefficient

$$C_T = \frac{T/A}{\frac{1}{2}\rho U^2} \tag{50}$$

where U is the local blade speed and T/A is the thrust per unit area at that radius of the actuator disk. The local advance coefficient is

$$\phi = (V_0/U) \tag{51}$$

Figure 11 would normally be generated from tests or analyses of a free-running propeller with undistorted inflow. We can use it, however, to estimate what would happen if locally around the circumference the inflow velocity was reduced by dV_0 as in a body wake. The increase in local thrust coefficient would affect the jet velocity V_j. Referring back to Eq. (16), we see that the wake recovery would then be given by

$$R = 1 - \frac{dV_j}{dV_0} \tag{52}$$

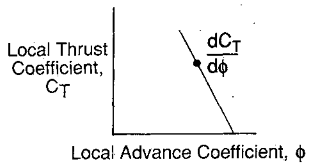

Fig. 11 Propeller blade element characteristic.

Using Eqs. (1) and (3), Eq. (50) becomes

$$C_T = [(V_j^2 - V_0^2)/U^2] \tag{53}$$

Differentiation of Eqs. (53) and (51) with U constant then allows Eq. (52) to be written

$$R = 1 - \frac{2\phi + (dC_T/d\phi)}{2\sqrt{\phi^2 + C_T}} \tag{54}$$

which can be used when the element characteristics are known.

The analyses in the following three sections can provide some guidance for cases for which the local element characteristics are not known.

B. Lightly Loaded Single-Rotation Propeller

The restriction to light loading is a consequence of the assumption that the static pressure in the jet is the ambient value. The swirl component velocity V_u is included in the analysis to obtain the wake recovery, although the wake recovery definition involves only the axial component V_j.

The power added per unit mass flow is, according to the Euler equation of turbo-machinery

$$P/\dot{m} = UV_u \tag{55}$$

This power is absorbed by the fluid and shows up as an increase in stream kinetic energy

$$P/\dot{m} = \tfrac{1}{2}(V_j^2 + V_u^2 - V_0^2) \tag{56}$$

Equating these powers, and employing the geometry of the velocity triangles at the actuator disk shown in Fig. 12, we can obtain

$$V_j^2 + \tfrac{1}{4}(V_j + V_0)^2 \cot^2\varphi_2 - V_0^2 = U^2 \tag{57}$$

This will be differentiated to obtain dV_j/dV_0 for substitution into Eq. (52) to obtain R. We will also employ

$$\nu = \frac{d\cot\varphi_2}{d\cot\varphi_1} \tag{58}$$

where ν is a constant depending on cascade geometry. Using Weinig's flat plat cascade theory[8] the author has found to good approximation

$$\nu = \exp\left[-\pi\sigma\left(\sin\varphi^* + \frac{1 - \sin\varphi^*}{1.28}\sigma^{\csc\varphi^*}\right)\right] \tag{59}$$

where φ^* is the zero-lift direction and σ is the cascade solidity as shown in Fig. 12.

Eq. (57) is now differentiated with U constant using Eq. (58) and

$$\cot\varphi_1 = [2U/(V_j + V_0)] \tag{60}$$

After much algebra, and also using Eqs. (51–53), we obtain

$$R = \frac{2(1 - \nu\sqrt{1 - C_T}) - C_T}{1 - \nu\sqrt{1 - C_T} + \phi^2 + \phi\sqrt{\phi^2 + C_T}} \tag{61}$$

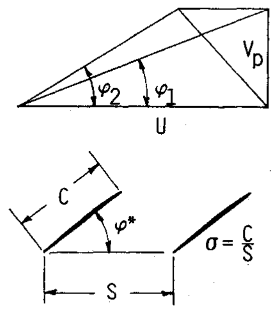

Fig. 12 Velocity triangles at actuator disk and blading cascade parameters.

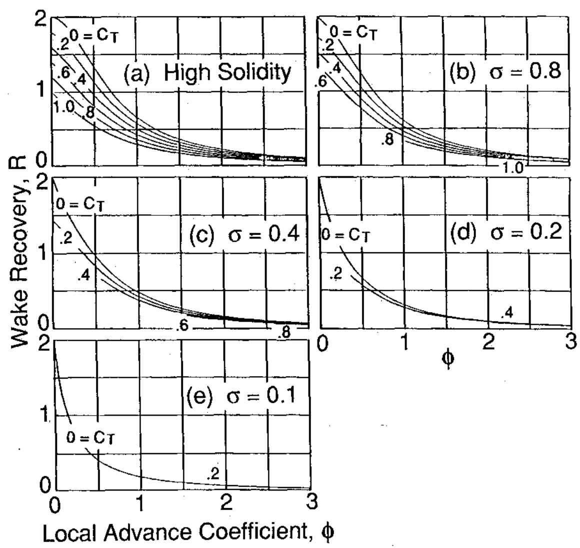

Fig. 13 Wake recovery for single-rotation propeller blade elements.

This result is shown graphically in Fig. 13. In constructing Fig. 13 it was assumed for simplicity that $\varphi^* = \varphi_2$, and since φ_2 can be determined from ϕ and C_T, R depends only on ϕ, C_T, and σ. The airfoil lift coefficient can also be calculated from these variables, and the lines in the figure have been terminated at the locations where the lift coefficient reaches unity.

The most noteworthy feature of Fig. 13 is that the wake recoveries fall off to low values at high advance coefficients. This means that the hub elements of single-rotation propellers will have poor recoveries because of their low blade speeds. Downstream part-span stator vanes could be used to improve recoveries there, and they do not necessarily need to be placed around the whole circumference, but perhaps just in the wake region.

C. High Solidity Counter-Rotating Propellers

For simplicity, we assume that the blade speeds are equal and that the two rotors are very close together so that there is no change in properties between the two actuator disks. We proceed as in Sec. IV.B. and arrive at an equation analogous to Eq. (57) except that it is more complex and contains the exit flow angle from the aft rotor as well as that from the forward rotor. Because of the complexity we assume that the exit flow angles remain constant as V_0 is varied; thus the result applies only to rotors that have high solidity. The final expression simplifies to

$$R = \frac{12}{6 + (\phi + \sqrt{\phi^2 + C_T})^2} \tag{62}$$

This is plotted in Fig. 14. Although the downward trend with increasing advance coefficient is still apparent, the wake recovery values are considerably higher than for high-solidity single-rotation propellers at representative advance coefficients and thrust coefficients.

D. Wake Recovery for Thin Shallow Inviscid Wakes

In the preceding sections the wake fluid has been assumed to be guided by the blading in the same way as the freestream fluid. A better approximation for cases in which the wake is thin compared to the blade spacing is given in this section. The approach used is that described by Smith[9] and it is shown in Fig. 15. Because of the circulation around the airfoils, particles traverse the suction side faster than the pressure side, and a wake turns into disconnected segments as it passes through a rotor.

Across the rotor we assume the flow is two-dimensional, and therefore, the vorticity in the wake, which is perpendicular to the figure, remains constant as the particles proceed. Consider the fluid in a segment of the wake *A-B* upstream. Later that same fluid appears as segment *C-D* downstream. Since the segment length has increased, its width has decreased proportionately, and with constant vorticity the wake velocity defect has decreased because it is proportional to the wake width. Formulas given previously by the author[10] can be used to deduce the segment length increase. This is a piece of the wake recovery, but we need to also consider wake changes in the upstream and downstream regions where the flow is accelerating. In those regions it is appropriate to assume that the flow is accelerating because the stream surfaces are contracting and, therefore, the flow is not two-dimensional and the vorticity is not constant. But we can use the Helmholz law that states that the vorticity is proportional to the vortex line length, which is proportional to the streamtube lamina thickness, which is inversely proportional to the axial velocity. By also assuming that for shallow wakes the tangential component of the wake width is constant in these regions, we can calculate the wake velocity defect changes there. Only the axial component of the final wake defect in the jet is used to calculate R.

The analysis just outlined and the final expressions are rather complex and will not be given here. Figure 16 presents the results obtained. It is interesting to note that the recovery is now increased with increased loading. That is because the

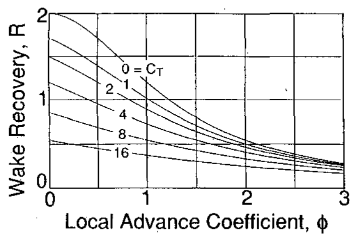

Fig. 14 Wake recovery for high solidity counter-rotating propeller blade elements.

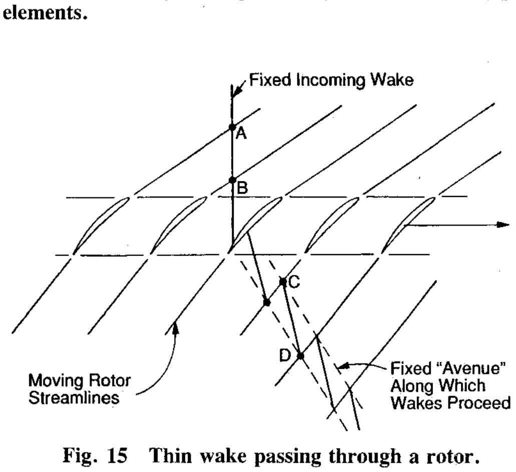

Fig. 15 Thin wake passing through a rotor.

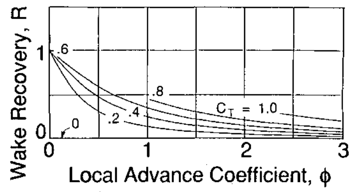

Fig. 16 Wake recovery for single-rotation propeller blade elements ingesting thin, shallow, inviscid wakes.

wake fluid is now deflected by the potential flow pressure field of the rotor blades rather than being guided by the blade surfaces. The blade chord length does not enter the analysis, only the blade circulation and blade spacing. However, it is unreasonable to use this method with high solidity because then the assumption that the blade surfaces don't guide the flow would clearly be invalid. The lines on the figure have arbitrarily been terminated for a lift coefficient of unity with a solidity of 0.8.

V. Method for Application

In conducting the analyses it was assumed that the static pressure was constant across the wake, and that the velocity variation in the wake was caused by viscous rather than potential field effects. In actual applications there will be a static pressure field in the wake at the location where the propulsor is to be placed (and a different static pressure field there when the propulsor is in place and operating). Because of these pressure fields, the actual wake velocity distributions are insufficient and inconvenient for use in our analysis, which is basically concerned with energy fluxes.

When designing a propulsor for a craft for which there will be significant wake ingestion, such as a torpedo or cruise missile, the first step is to determine the flowfield at the location where the propulsor is to be placed either from model tests or from a viscous flow analysis. The most important property of the flowfield at the propulsor location is the distribution of total pressure, because that relates to the viscous losses that have occurred. A procedure for applying this information is given in Fig. 17.

Note in step 1 in Fig. 17 that the procedure can be applied using data either with (or without) the propulsor present. This choice implies that the result will be the same in either case. The result will only be the same if the potential field of the propulsor has not affected the upstream viscous losses. This is an important point because often the acceleration of the flow into the propulsor will prevent or minimize flow separation losses on craft with blunt afterbodies. (On the other hand, it is conceivable that craft with fine afterbodies could have their viscous drag increased by increased skin friction ahead of the propulsor.) In fact, we can conceive of designing blunt craft that only avoid massive flow separation because their propulsors ingest their boundary layers (Wislicenus[2,3]). So we should use wake data obtained with the actual (or a similar) propulsor in place if they are available, and recognize that if we use unpropelled data because they are all that are available, we are tacitly assuming that the presence of the propulsor will not affect the craft's viscous drag.

It should be emphasized that any benefit in craft viscous drag reduction resulting from wake ingestion is in addition to the benefit described in this article.

When a propulsor is added to a craft it changes the pressure field on the body surface, and therefore, one might say it changes the craft's drag. From a propulsive efficiency standpoint this is neither bad nor good, since the momentum and energy fluxes far downstream and the corresponding far upstream fluxes determined as outlined in Fig. 17 determine the propulsive thrust and propulsive power that determine the propulsive efficiency. For structural design purposes it is important to know where the forces occur, but for the propulsive efficiency determination it is not. It is noted in passing that in the marine propulsion community it is commonplace to use

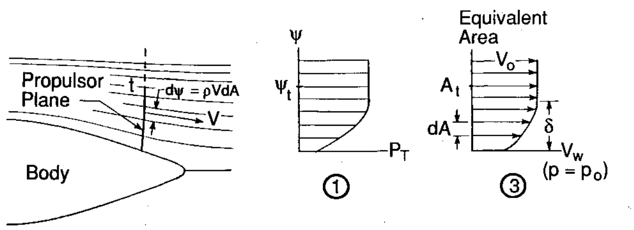

① Establish total pressure vs. streamfunction at propulsor plane with (or without) propulsor present from measurement or viscous analysis.

② Calculate velocity V_w assuming ambient static pressure in wake.

③ Distribute V_w over equivalent area using $dA = \frac{d\psi}{\rho V_w}$.

④ Determine $\delta*$, θ, k from distribution of ③.

Fig. 17 Procedure for applying measured or calculated wake data.

the term "thrust deduction" to represent the drag increase of the craft associated with the flow induction field of the propulsor and the corresponding thrust increase needed on the propulsor to balance it.

In Fig. 17, the streamline that passes the tip of the propulsor disk has been indicated with the symbol t. Although the total pressure distribution shown in panel 1 and the velocity distribution in panel 3 should not be much different whether or not the propulsor is in place, the tip stream function will be different, and so will be the tip equivalent area. The ratio of the tip equivalent area without the propulsor in place to the actual area is a measure of the potential field of the basic body since it only differs from unity because the static pressure is different from ambient. It is recommended that this ratio be applied to the actual area to obtain the A used in this article.

VI. Summary and Conclusions

A method is presented for estimating the amount of propulsive power that can be saved when the viscous wake of a body is used as part of the propulsive fluid. The propulsive power is represented by the axial kinetic energy flux in the downstream wake, assuming that the wake is at ambient static pressure. The propulsive power is related to the actual shaft power through the axial kinetic energy efficiency, which accounts for blading and other propulsor surface viscous and shock losses, induced losses for open-tip propulsors, and wake swirl kinetic energy losses. Except for single-rotation propellers where swirl losses might change significantly, the axial kinetic energy efficiency should not be greatly affected by wake ingestion, so a percentage reduction in propulsive power should be nearly realized as a reduction in shaft power.

Results are presented in two formats: 1) a power-saving coefficient, and 2) a propulsive efficiency with wake ingestion. The power-saving coefficient is perhaps more useful when assessing wake ingestion from appendages such as support struts, whereas the propulsive efficiency is more applicable to cases when a large part of the craft's viscous wake is ingested. Significant power savings are found for certain cases.

Several conclusions can be drawn from the numerical results.

1) The power saving with wake ingestion is greatest for small propulsors, i.e., propulsors with high thrust-loading coefficients.

2) The power saving is greatest when the form factor of the wake being ingested is high. This means that the propulsor should be positioned so that it ingests the wake before the wake is flattened much by fluid shear stresses.

3) The flattening of the wake by reversible energy addition of the propulsor is favorable. This is a property of the propulsor named wake recovery. Although high wake recovery is favorable, it is not found to be of major importance. Methods for estimating the wake recoveries of propeller-type blade elements are given. It is found that the local advance ratio (ratio of forward speed to local blade speed) is the dominant parameter. High advance ratios, such as occur near the hub, are unfavorable.

A procedure is given for interpreting and applying wake data from measurements or viscous analyses at the propulsor location on a craft. The effects of the static pressure field induced by the propulsor are discussed. It is pointed out that any benefit resulting from the reduction of boundary-layer flow separation losses by this pressure field is in addition to the benefit described in this article.

VII. Appendix: Small Wake Extreme

As $D/T \to 0$, $(V_j' - V_j) \to 0$ and the first term in Eq. (27) becomes indeterminant. But then Eq. (28) can be written, using the binomial expansion

$$V_j' - V_j = (V_0^2/V_j)(\theta/A)R - [(V_j^2 - V_0^2)/2V_j](\delta_p^*/\theta)(\theta/A) \qquad \text{(A1)}$$

and using Eq. (29)

$$(V_j' - V_j)\frac{T}{D} = \frac{V_0^2}{V_j}\left[R - \frac{1}{2}\left(\frac{V_j^2}{V_0^2} - 1\right)\frac{\delta_p^*}{\theta}\right] \cdot \frac{\frac{1}{2}[(V_j^2/V_0^2) - 1]}{1 - R(D/T) + \frac{1}{2}[(V_j^2/V_0^2) - 1](\delta_p^*/\theta)(D/T)} \qquad \text{(A2)}$$

which can be used together with Eq. (36) in the first term of Eq. (27).

Acknowledgments

The author would like to thank Donald M. Hill who performed the numerical analyses, Robert Henderson, Walter Gearhart, Justin Kerwin, Edward Greitzer, and William Morgan who provided helpful discussions and references, and GE Aircraft Engines for permission to publish this article.

References

[1]Betz, A., *Introduction to the Theory of Flow Machines*, Sec. 59, First English Edition, Pergamon, New York, 1966, pp. 215–217.

[2]Wislicenus, G. F., and Smith, L. H., "Hydraulic Jet Propulsion and Incipient Cavitation," Internal Flow Research Rept. I-6, Pt. A, Johns Hopkins Univ., Mechanical Engineering Dept., Baltimore, MD, March 21, 1952.

[3]Wislicenus, G. F., "Hydrodynamics and Propulsion of Submerged Bodies," *Journal of the American Rocket Society*, Vol. 30, Dec. 1960, pp. 1140–1148.

[4]Gearhart, W. S., and Henderson, R. E., "Selection of a Propulsor for a Submersible System," *Journal of Aircraft*, Vol. 3, No. 1, 1966, pp. 84–90.

[5]Bruce, E. P., Gearhart, W. S., Ross, J. R., and Treaster, A. L., "The Design of Pumpjets for Hydrodynamic Propulsion," NASA SP-304, Pt. II, 1974, pp. 795–839.

[6]McCormick, B. W., *Aerodynamics of V/STOL Flight*, Academic Press, New York, Chap. 4

[7]Lieblein, S., and Roudebush, W. H., "Low-Speed Wake Characteristics of Two-Dimensional Cascade and Isolated Airfoil Sections," NASA TN 3771, Oct. 1956.

[8]Weinig, F. S., *Die Strömung um die Schaufeln von Turbomaschinen*, J. A. Barth, Leipzig, Germany, 1935.

[9]Smith, L. H., "Wake Dispersion in Turbomachines," *Journal of Basic Engineering, ASME Transactions*, Vol. 88, Ser. D, No. 3, 1966, pp. 688–690.

[10]Smith, L. H., "Secondary Flow in Axial-Flow Turbomachinery," *ASME Transactions*, Vol. 77, No. 7, 1955, pp. 1065–1076.